The Journal of Neuroscience, July 1, 1998, *18*(13):4993–5007

$GABA_A$ Receptor Pharmacology and Subtype mRNA Expression in Human Neuronal NT2-N Cells

Torben R. Neelands,[1] L. John Greenfield Jr,[2] Jie Zhang,[1,2] R. Scott Turner,[1,2,4] and Robert L. Macdonald[1,2,3]

[1]Neuroscience Program and Departments of [2]Neurology and [3]Physiology, University of Michigan, and [4]Veterans Affairs Medical Center Geriatric Research, Education, and Clinical Center, Ann Arbor, Michigan, 48104-1687

Human NT2 teratocarcinoma cells differentiate into neuron-like NT2-N cells when treated with retinoic acid. GABA evoked concentration-dependent whole-cell currents in NT2-N cells with an EC_{50} of 21.8 μM and a Hill slope of 1.2. $GABA_A$ receptor (GABAR) currents reversed at E_{Cl-} and did not display voltage-dependent rectification. GABAR single channels opened in bursts to a 23 pS main conductance level and a 19 pS subconductance level, with infrequent openings to a 27 pS conductance level. Kinetic properties of the main conductance level were similar to other native and recombinant GABAR channels. Diazepam and zolpidem enhanced GABAR currents with moderate affinity, whereas methyl-6,7-dimethoxy-4-ethyl-β-carboline-3-carboxylate inhibited GABAR currents. Loreclezole enhanced GABAR currents with high affinity, but furosemide antagonized GABAR currents with low affinity. The neurosteroids alphaxalone and pregnenolone sulfate appropriately modulated GABAR currents. Zinc blocked GABAR currents with low affinity, but lanthanum did not significantly alter NT2-N GABAR currents. Reverse transcription PCR (RT-PCR) performed on RNA from NT2-N cells clearly detected transcripts encoding human α2, α3, α5, β3, γ3, and π subtypes. The combined pharmacological and RT-PCR results are most consistent with a single or predominant GABAR isoform composed of an α2 and/or α3 subtype combined with the β3 and γ3 subtypes. The data do not rule out receptors containing combinations of α2 and/or α3 subtypes with the α5 subtype or receptors with both β1 and β3 subtypes. The presence or absence or the π subunit in functionally expressed receptors could not be determined.

Key words: GABA; electrophysiology; patch clamp; Ntera2; barbiturate; benzodiazepine; neurosteroid; single channel

GABA is the major inhibitory neurotransmitter in the vertebrate brain. Fast IPSPs are mediated by $GABA_A$ receptors (GABARs), which contain binding sites for many modulators including benzodiazepines, barbiturates, general anesthetics, penicillin, picrotoxin, bicuculline, and zinc. GABARs consist of five subunits that form a chloride ion channel. Four different subunit families (α, β, γ, and δ) have been studied extensively (Macdonald and Olsen, 1994), and two new subunit families, π (Hedblom et al., 1997) and ϵ (Davies et al., 1997), have been identified recently. In addition, in mammals, including humans, six α (α1–α6), three β (β1–β3), and three γ (γ1–γ3) subtypes have been described. Pharmacological studies of recombinant receptors have shown that individual subunits and their subtypes confer different sensitivities to GABAR modulators such as benzodiazepines (Pritchett et al., 1989; Wieland et al., 1992) and zinc (Draguhn et al., 1990). The subunit subtypes are differentially expressed throughout development and in different CNS regions (Wisden et al., 1992), reducing the total number of possible isoforms that can be formed in different brain regions and in individual cells.

Studies of GABARs in human CNS neurons have been difficult because of heterogeneity of cell types and unknown GABAR subtype expression. For example, in isolated human central neurons, the heterogeneity of cell types has led to a wide range of responses to GABAR modulators, presumably because of differing subunit composition (Gibbs et al., 1996). It has not been possible to isolate a homogeneous population of postmitotic neurons from human brain and maintain them in culture for detailed pharmacological and biochemical studies. Electrophysiological studies of neuronal GABARs, therefore, have relied on nonhuman neurons in primary cell cultures or acutely isolated neuron preparations. However, the transcriptional, translational, and post-translational processing, assembly, transport, and subcellular localization performed by a heterogeneous population of rodent neurons may not adequately reflect the behavior of human neurons.

The NT2-N human neuronal cell line offers a useful bridge between studies of defined recombinant receptors expressed in non-neuronal cell lines and studies of native nonhuman receptors. Prolonged treatment of the human NT2 teratocarcinoma cell line with retinoic acid causes these pluripotential cells to become terminally differentiated into neurons termed NT2-N cells (Pleasure et al., 1992). After differentiation, NT2-N cells extend both dendritic and axonal processes and express neuron-specific cell surface, cytoskeletal, and secretory markers and functional neurotransmitter receptors (Pleasure et al., 1992; Younkin et al., 1993; Munir et al., 1995; Beczkowska et al., 1997). Levels of protein kinases A and C have also been shown to increase in NT2 cells during differentiation (Abraham et al., 1991), which may be important in regulating the function of these receptors and other cellular processes. In addition, recent reports have shown the existence of synaptic connections between cells in culture (Hartley et al., 1997). In this study we demonstrated that NT2-N cells expressed functional human GABARs with relatively homogeneous properties, suggesting that NT2-N cells may provide a useful model system for investigation of human GABARs assem-

Received Nov. 11, 1997; revised April 14, 1998; accepted April 17, 1998.

We thank Nadia Esmaeil and Yunning Yang for their technical support in differentiating and maintaining the NT2-N cells and Dr. Ewen Kirkness for contribution of π cDNA, which was used as positive controls in the RT-PCR experiments.

Correspondence should be addressed to Dr. Robert L. Macdonald, Neuroscience Laboratory Building, 1103 East Huron Street, Ann Arbor, Michigan, 48104-1687.

 0270-6474/98/184993-15$05.00/0

bled and expressed in a homogeneous population of human neurons.

MATERIALS AND METHODS

Cell culture. NT2 cells were grown and maintained in DMEM high glucose (HG) with 10% fetal bovine serum, and penicillin and streptomycin were added as previously described (Andrews, 1984). Cells were plated at 2×10^6 cells/75 cm^2 flask and differentiated by treatment with 1 μM retinoic acid (RA) for 4 weeks. After RA treatment, cells were washed with versene and then treated with trypsin to dislodge the cells. Cells were resuspended after being triturated and replated at a 1:10 dilution with DMEM HG and maintained in 5% CO_2. The following day the media was removed and saved as conditioned media to feed replates II and III. Cells were again treated with trypsin and then spun for 5 min at 1000 rpm. The pellet was resuspended in 1 ml of media containing mitotic inhibitors (in μM: 10 5-fluoro-2′deoxyuridine plus 10 uridine and 1 cytosine arabinoside) and replated (replate II). The same treatment was performed again after 1 week in culture (replate III) to obtain ~100% pure neurons. These cells were replated onto 35 mm Corning (Corning, NY) dishes for electrophysiological recording. For these experiments we limited selection of cells to those that were isolated and had neuronal morphology. NT2-N cells tend to form clusters as they differentiate in culture, and cell–cell interactions could possibly effect the differentiation process and resulting cell morphology and might affect neuronal properties. In addition, cell cultures were at best only 99% pure neurons. The contaminating non-neuronal cells were morphologically distinct and could be eliminated by visual selection for electrophysiological experiments.

Solutions and drug application. Cells were removed from the 5% CO_2 incubator, and the feeding medium was replaced with recording medium (in mM: 142 NaCl, 1 $CaCl_2$, 6 $MgCl_2$, 8.09 KCl, 10 glucose, and 10 HEPES, 315–325 mOsm, pH 7.4). Patch-clamp electrodes of 5–10 MΩ were filled with pipette solution (in mM: 153.33 KCl, 1 $MgCl_2$, 10 HEPES, 5 EGTA, and 2 ATP, 300–310 mOsm, pH 7.3). This combination of solutions results in nearly equivalent intracellular and extracellular chloride ion concentrations, hence an E_{Cl-} of ~0 mV, and produced an inward current when cells were voltage clamped at negative potentials.

Compounds were applied to cells using a modified U-tube "multipuffer" application system (Greenfield et al., 1996). The U-tube system enabled us to position a micropipette with a 40–50 μm tip next to the cell for the duration of the recording and apply multiple concentrations of individual drugs to each cell. Stock solutions of GABA, diazepam, lanthanum, pentobarbital, phenobarbital, picrotoxin, 3-5-pregnen-3β-ol-20-one sulfate sodium salt (pregnenolone sulfate), zinc, and zolpidem were made by dissolving each in sterile water. Stock solutions of (3α)-hydroxy-(5α)-pregnan-11,20-dione (alphaxalone), bicuculline, methyl-6,7-dimethoxy-4-ethyl-β-carboline-3-carboxylate (DMCM), furosemide, and loreclezole were dissolved in dimethylsulfoxide (DMSO) and diluted with sterile water (final DMSO concentration was <0.1% v/v). Individual drugs were diluted in recording medium to their final concentration. Alphaxalone and pregnenolone sulfate were purchased from Research Biochemicals (Natick, MA). Loreclezole was obtained from Janssen Biochimica (Berse, Belgium). Bicuculline was purchased from Calbiochem (La Jolla, CA). All other compounds were from Sigma (St. Louis, MO).

Electrophysiology. Whole-cell voltage-clamp and single-channel recordings using the patch-clamp technique were obtained as described previously (Hamill et al., 1981). Patch-clamp electrodes were pulled from Labcraft microhematocrit capillary tubes (Curtin Matheson Scientific, Inc., Houston, TX) or WPI (Sarasota, FL) borosilicate electrode glass (1B150F-3) using a Flaming-Brown P-87 micropipette puller (Sutter Instrument Co., San Rafael, CA). Borosilicate pipettes were fire-polished on a Narashige MF-3 microforge and subsequently coated with polystyrene Q-dope (GC Electronics, Rockford, IL) to reduce electrode tip capacitance.

Whole-cell recordings were performed using an Axopatch 1-B amplifier (Axon Instruments, Foster City, CA). Signals were digitized on-line at 200 Hz using a Labmaster TL-1 analog-to-digital converter (ADC), recorded, and subsequently analyzed off-line using Axotape 2.0 software (Axon Instruments). Single-channel recordings were obtained from "outside-out" patches formed using standard techniques (Hamill et al., 1981) with an Axopatch 200A amplifier. Single-channel currents were low-pass-filtered at 2 kHz using an eight pole Bessel filter and subsequently digitized on line at 20 kHz using Axotape 2.0 software. For some later patch recordings, digitization was performed using a Digidata 1200A ADC and Axoscope software (Axon Instruments).

Data analysis. The magnitude of the enhancement or inhibition of GABAR current by a drug was measured by dividing the peak amplitude of GABAR currents elicited in the presence of a given concentration of the drug (with GABA) by the peak amplitude of control current elicited by GABA alone and multiplying the fraction by 100 to express it as percent of control. Thus the control response was 100%. Peak GABAR currents at various drug concentrations were fitted to a sigmoidal function using a four-parameter logistic equation (sigmoidal concentration–response) with a variable slope. The equation used to fit the concentration–response relationship was:

$$I = \frac{I_{max}}{1 + 10^{(\mathrm{Log}_{EC50} - \mathrm{Log}_{drug}) * \mathrm{Hill\ slope}}}$$

where I was the GABAR current at a given GABA concentration, and I_{max} was the maximal GABAR current. Maximal current and concentration–response curves were obtained after pooling data from all cells tested for GABA and for all drugs. Concentration–response curves were also obtained from individual cells. The curve-fitting algorithm minimized the sum of the squares of the actual distance of points from the curve. Convergence was reached when two consecutive iterations changed the sum of the squares by <0.01%. The curve fit was performed on an IBM PC compatible personal computer using Prism 1.0 or 2.0 (Graph Pad, San Diego, CA). Data are presented as mean ± SEM.

To quantify whole-cell current rectification, peak amplitudes of responses to GABA (at EC_{50} concentrations) were measured at holding potentials of −50 and +50 mV. These responses exhibited no visible desensitization. An amplitude ratio (+50:−50 mV) was calculated, and rectification was determined with respect to a linear ratio of 1.0 using the predicted E_{Cl} of 0 mV. An amplitude ratio >1.0 indicated outward rectification. To quantify voltage-dependent differences in desensitization, the amount of desensitization produced by a high concentration of GABA (100 μM) was first determined at holding potentials of −50 and +50 mV. Desensitization was expressed as (1 − amplitude at end of GABA application)/(peak GABA amplitude). A desensitization ratio (+50:−50 mV) was then calculated using the method used to characterize rectification. A desensitization ratio <1.0 was indicative of less desensitization at depolarized membrane potentials.

Single-channel current analysis. Analysis of single-channel currents off-line consisted of amplitude and interval detection with Fetchan 6.0 (Axon Instruments) using a 50% threshold detection system, followed by pStat 6.0 (Axon Instruments) for amplitude histograms, and subsequent kinetic investigation using Interval 5 (Dr. Barry S. Palotta, University of North Carolina, Chapel Hill, NC) and software developed in our laboratory (Macdonald et al., 1989). To reduce errors resulting from multichannel patches, recordings were included in the kinetic analysis only if overlaps of simultaneous openings were very brief and occurred in <1% of openings. Open and shut duration histograms were constructed as described by Sigworth and Sine (1987) and fit by the maximum likelihood method. The number of exponential functions required to fit the binned data was increased until additional components did not significantly improve the fit, as determined by the log-likelihood ratio test (Horn 1987; McManus et al., 1988). Intervals with durations <1.5 times the system dead time were displayed in the interval histograms but not included in the fit. Bursts were defined as clusters of openings separated by closures longer than the two shortest closed components, which were thus considered intraburst closures. A critical gap for each patch was calculated from the closed interval distribution to equalize the proportion of misclassified events (Colquhoun and Sakmann, 1985). Prolonged (30 sec to several minutes) drug applications were used to ensure stationarity of channel activity.

Reverse transcription PCR. Total RNA was isolated from NT2-N neurons using the Ultraspec method by Biotecx (Houston, TX). One microgram of total RNA was treated with DNase in a total volume of 10 μl composed of 1 μl of 10× DNase I buffer, 1 μl of DNase I (1 U/μl), and 7 μl of DEPC water. This mixture was incubated for 15 min at 25°C. Addition of 1 μl of 25 mM EDTA was followed by a 10 min incubation at 70°C to heat inactivate the DNase I. The reaction mixture was then chilled immediately on ice. One microliter of a random primer (0.6 μg/μl) was then added to the mixture that was then incubated at 25°C for 15 min. Reverse transcription used the product of the above reaction mixed with the following: 1 μl of 5× first-strand buffer, 2 μl of 0.1 M DTT, 1 μl of 10 mM dNTP mix, and 1 μl of RNase inhibitor (10 U/μl).

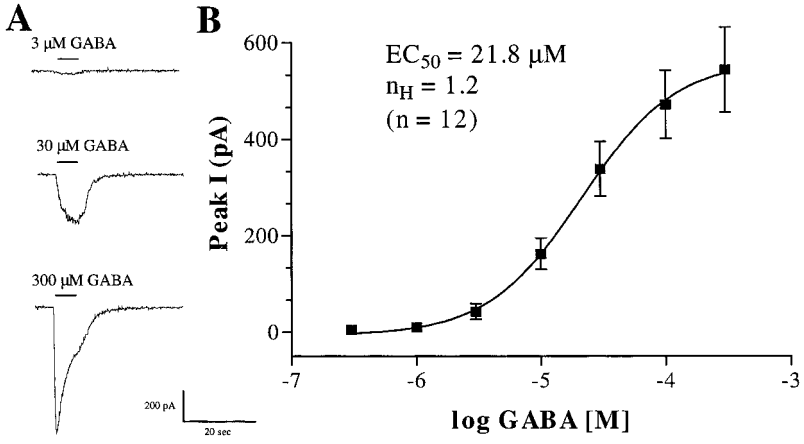

Figure 1. GABA concentration–response characteristics for NT2-N cell GABARs. *A*, Representative traces of GABAR responses to increasing concentrations of GABA ($V_h = -75$ mV). *Horizontal bar*, GABA application (3, 30, or 300 μM). *B*, Concentration–response curve of average peak GABA-evoked currents ($n = 12$) fitted with a four-parameter logistic equation. Data are mean ± SEM.

The mixture was prewarmed for 2 min at 42°C before addition of 1 μl of Superscript II (10 U/μl) and then was incubated for 45 min at 42°C. Using the same procedure as described above, with the exception that 1 μl of DEPC water was substituted for Superscript II, acted as a negative control. The reverse transcription product was heat-inactivated for 15 min at 70°C before PCR. The PCR reaction was performed for each subunit in 100 μl of the following mixture: 1 μl of a 20 μM primer mixture (3′ primer and 5′ primer), 2 μl of the reverse transcription product, 10 μl of 10× buffer, 16 μl of 25 mM $MgCl_2$, 1 μl of 25 mM dNTP mixture, 0.5 μl of Amplitaq (Perkin-Elmer, Norwalk, CT; 5 U/μl), and 72.5 μl of DEPC-treated water. The templates for the PCR reaction using cDNA for each subunit subtype were used as positive controls. PCR was performed as follows: a 2 min period at 94°C to denature the mixture, 35 cycles at 94°C for 1 min, 55°C for 2 min, 72°C for 1 min, and a 7 min extension period at 72°C. PCR products (5 μl for positive controls, 15 μl for both test and negative controls) were mixed with dye and run on a 1.5% agarose gel at 120 V for 40 min and then stained with ethidium bromide and photographed. Reaction reagents were purchased from Amplitaq; random primer, Superscript II, RNase inhibitor, and DNase I were purchased from Life Technologies (Gaithersburg, MD); and dNTP mix and DNA molecular weight marker VI were purchased from Boehringer Mannheim (Indianapolis, IN).

RESULTS

NT2-N cell GABAR current

NT2-N cells were voltage-clamped in the whole-cell configuration. Neurons can first be isolated 5 weeks after retinoic acid treatment has begun (Pleasure et al., 1992). At this time multipolar cells were the predominant cell type found in the cultures, and they were readily identifiable. Immediately on rupturing the membrane for intracellular access, the resting membrane potential was measured for each NT2-N cell by shifting to current-clamp mode with current set at zero. Resting membrane potentials ranged from −49 to −33 mV with an average of −40.9 ± 0.4 mV ($n = 118$). Cells were then voltage-clamped at −75 mV, and 300 μM GABA was applied for 6–10 sec to determine whether functional GABARs were expressed on the membrane surface. Whole-cell currents resembled those seen in recordings of native GABARs in mouse cortical neurons (Kume et al., 1996) and recombinant receptors (Angelotti et al., 1993) with a rapid concentration-dependent rising phase, followed by a decrease in current (despite continued application of GABA), consistent with desensitization. The apparent desensitization occurred at GABA concentrations >10 μM and was typically monoexponential in time course, with faster rates at increased GABA concentrations. Typical current traces from an NT2-N cell are shown in Figure 1*A*. Peak amplitudes of NT2-N cell responses ($n = 12$) to a range of GABA concentrations (300 nM to 300 μM) were pooled and fitted to a sigmoidal logistic function (EC_{50}, 21.8 μM; Hill slope, 1.2) (Fig. 1*B*). Individual EC_{50} values ranged from 7 to 80 μM with an average of 31.3 ± 8.3 μM. NT2-N cells had an average maximal current of 472.4 ± 70.5 pA at 300 μM GABA ($n = 12$).

Voltage dependence of GABAR currents

The degree and direction of GABAR current rectification depended on the GABAR isoform (Burgard et al., 1996). Whole-cell current–voltage (*I–V*) relations were generated in NT2-N cells by measuring peak currents evoked by 30 μM GABA at holding potentials from −100 to +75 mV at 25 mV increments. In all cells studied ($n = 6$), there was no evidence of inward or outward current rectification. A plot of the average peak current at each holding potential for the four cells in which the complete *I–V* relations were generated resulted in a linear *I–V* plot ($p < 0.001$) (Fig. 2). An amplitude ratio of 0.90 ± 0.90 was calculated for six cells by dividing the peak current evoked at +50 mV by the peak current evoked at −50 mV. This again indicates that there was no rectification in either direction, because the amplitude ratio was not significantly different from unity (see Materials and Methods).

Voltage-dependent desensitization to high concentrations of GABA was also dependent on the GABAR isoform expressed (Burgard et al., 1996). In the continued presence (15 sec) of 100 μM and higher GABA concentrations, there was a prominent exponential decrease in amplitude from peak until the agonist was removed. The rate of apparent desensitization increased with higher GABA concentration. With our application system, rapid desensitization (time constants <50 msec) could not be recorded, but slower desensitization (time constants >100 msec) could be characterized. To determine whether this apparent desensitization was voltage-dependent, cells were held at +50 and −50 mV for sequential 15 sec applications of 100 μM GABA. The current amplitude at the end of the application was divided by the peak (initial) current for each holding potential. The desensitization ratio for the four cells tested was 1.01 ± 0.12 (see Materials and Methods), indicating no voltage dependence of desensitization during applications of 100 μM GABA at these holding potentials.

Single-channel currents

Single-channel currents were recorded in the outside-out configuration from a total of 116 GABA applications onto 19 excised patches in six separate experiments. However, most of these patches were not used for kinetic analysis because of the large number of overlapping or multiple openings, suggesting a high density of GABAR channels in the NT2-N cell membrane. Five

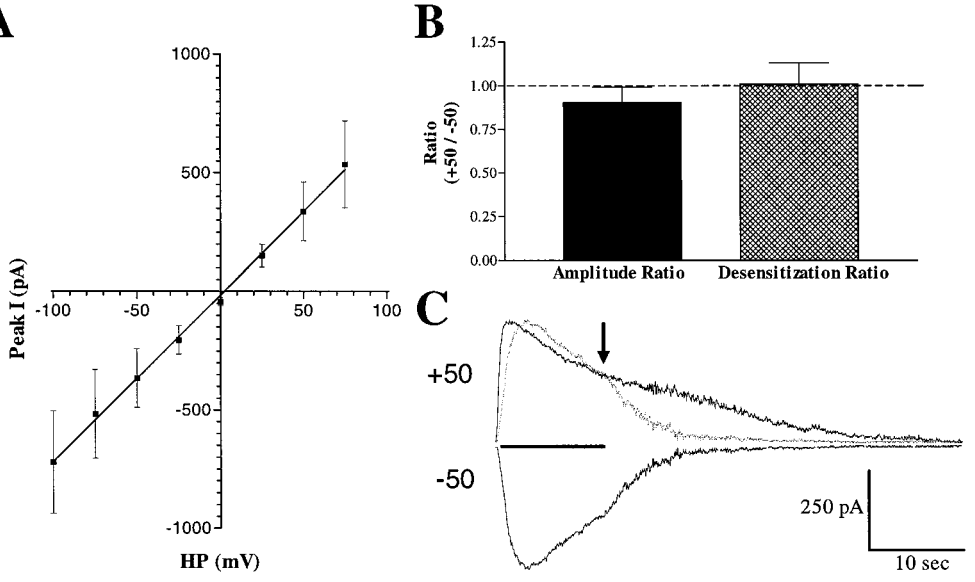

Figure 2. Voltage-dependent properties of NT2-N cell GABARs. *A*, Current–voltage relationship for five NT2-N cells. Peak currents evoked by 30 μM GABA, represented as mean ± SEM, are plotted against holding potential showing no rectification. *B*, NT2-N cells show no rectification or voltage-dependent desensitization. Amplitude ratio (*filled bar*) and desensitization ratio (*hatched bar*) were not significantly different from 1. Bars represent mean ± SEM. Larger amplitude ratios indicate greater outward rectification, and larger desensitization ratios indicate more desensitization at positive membrane potentials. *C*, Membrane currents recorded in NT2-N cells in response to applications of 100 μM GABA (*horizontal bar*). Responses were obtained at V_h levels of both +50 and −50 mV. The response recorded at −50 mV has been inverted and superimposed on the +50 mV trace for comparison. The degree of desensitization was calculated by dividing the current remaining at the end of GABA application (*arrow*) by the peak response (see Materials and Methods).

patches were obtained in four of these experiments in which single openings predominated during applications of 1, 3, and 10 μM GABA. Data from these patches were used for most of the kinetic and amplitude analysis (see Materials and Methods).

GABAR single-channel currents opened singly and in bursts of multiple openings (Fig. 3*A*). At least two conductance levels were observed at most holding potentials: a main conductance level of 23 pS in which the majority of openings were classified and a subconductance level of ~19 pS (Fig. 3*B*). Rare openings to a conductance level of ~27 pS were observed more commonly at negative than positive holding potentials. A current–voltage relationship was obtained by holding the membrane potential at voltages from −80 to +80 mV in 20 mV steps during sequential applications of 3 μM GABA. Openings were detected using a 50% threshold based on the amplitude of the main (23 pS) conductance level and thus included both the subconductance (19 pS) and larger conductance level (27 pS) openings. Event amplitude histograms were best fit using three Gaussian functions; the statistical means of these functions for a single patch are displayed in the current–voltage relationship shown in Figure 3*B*. Linear regressions of mean amplitudes at each holding potential showed reversal of single-channel currents at ~0 mV for all three conductance levels, consistent with the reversal potential for chloride with these solutions. None of the three conductance levels demonstrated either inward or outward rectification at the holding potentials examined. An example of the amplitude histogram for openings in a different patch held at +50 mV (Fig. 3*C*) and −50 mV (Fig. 3*D*) demonstrates symmetrical conductance levels (i.e., no inward or outward current rectification), although the relative proportion of main to subconductance level openings was somewhat larger at more negative potentials. The relative proportion of 27 pS openings was small (5–10%) at both positive and negative holding potentials in most patches.

The frequency of single-channel openings increased with increasing GABA concentration, from 10.4 openings/sec during application of 1 μM GABA to 28.8 openings/sec with 10 μM GABA (Table 1). Mean open time also increased slightly from 1.4 to 1.6 msec, and the percentage of time open increased from 1.8 to 5.2%, consistent with both longer burst openings and increased opening frequency at increased GABA concentration. The mean closed time diminished as GABA concentration increased. Open-duration histograms from selected patches with minimal overlapping or multiple openings were fitted best with three exponential functions, suggesting three open time constants with durations of 0.2, 1.5, and 4.5 msec (Fig. 4*A*, Table 2). These time constants did not change significantly with GABA concentration, but the percentage of openings classified in each exponential distribution varied with GABA concentration. With 1 μM GABA, most of the openings were classified in the shortest (O1) distribution (57%) with smaller proportions of openings in the two longer opening classes (23% O2 openings and 12% O3 openings). As GABA concentration increased, the percentage of O1 openings decreased, and the percentage of longer openings increased (Fig. 4*A*), as predicted by models in which the binding of more than one GABA molecule drives the channel into longer open states (Macdonald et al., 1989). However, with 10 μM GABA, a concentration at which almost all openings would be expected to be in the O2 and O3 classes, there were still a large number of O1 openings. This may have resulted from "trapping" of liganded channels in a desensitized distal closed state, from which recovery was slow enough that brief applications of GABA (lasting 30–60 sec) were biased toward sampling channels in the O1 and O2 states.

Closed-duration histograms were fitted best with five exponential functions (Fig. 4*B*). As GABA concentration increased, the durations of the three longer closed states (C3, C4, and C5) decreased, whereas the durations of the two short states (C1 and C2) did not change (Fig. 4*B*). This was consistent with previous observations in our laboratory (Twyman et al., 1990; Angelotti and Macdonald, 1993) and the interpretation that the C1 and C2 states represent intraburst closures. Histograms of burst durations pooled for each GABA concentration (based on a critical gap determined for each patch) were fitted best with three exponential distributions whose time constants did not change significantly between 1 and 3 μM GABA (1.27, 3.07, and 24.4 msec for 1 μM GABA; 1.96, 2.32, and 24.7 msec for 3 μM GABA) (data not

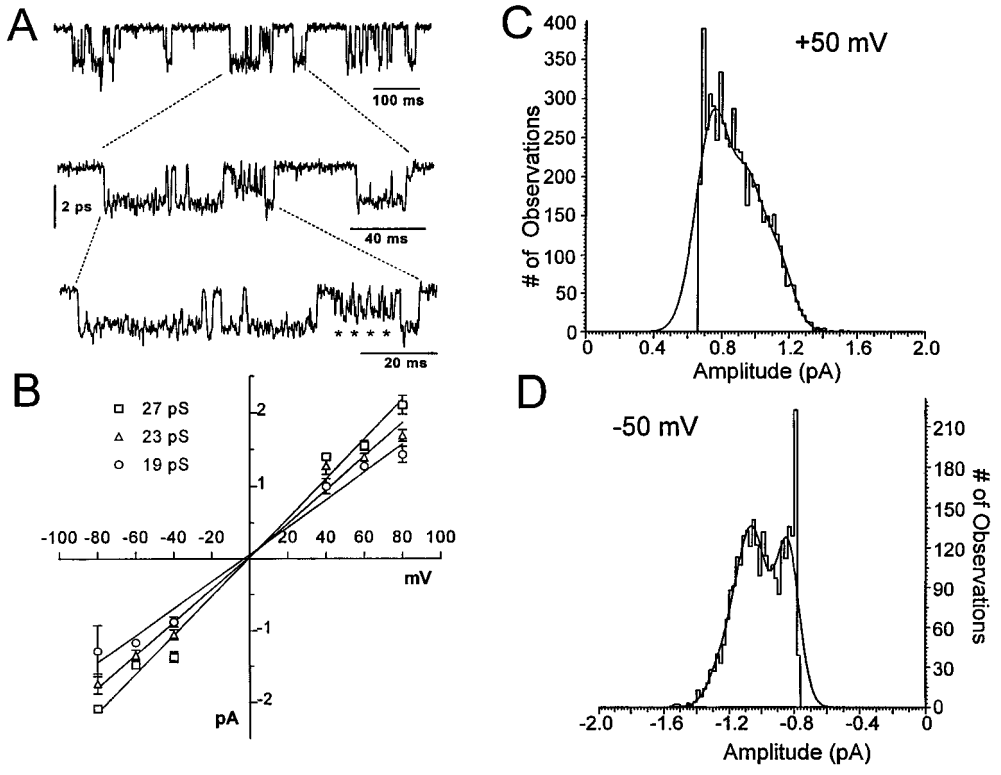

Figure 3. Single-channel currents obtained in the outside-out configuration from NT2-N cells. *A*, Representative raw data traces of channel openings in NT2-N cells illustrating the typical bursting pattern of openings to two different conductance states (openings to the subconductance state are indicated by *asterisks*). The same sample data are displayed on three different time scales (see calibration bars). *B*, Current–voltage relationship for single-channel currents evoked by 3 μM GABA. Amplitudes at each holding potential were obtained from amplitude histograms that were best fit with the means of three Gaussian distributions. *C, D*, Amplitude histograms of single-channel openings. The amplitudes of individual openings were measured and placed into 0.05 pA bins. The resulting frequency histograms were best fit with three Gaussian distributions of 27, 23, and 19 pS.

Table 1. Single-channel properties of NT2-N neurons

Property	GABA (1 μM)	GABA (3 μM)	GABA (10 μM)
Openings per second	10.4 ± 3.9	17.5 ± 3.6	28.8 ± 7.2
Mean open time (msec)	1.40 ± 0.12	1.53 ± 0.35	1.61 ± 0.20
Mean shut time (msec)	126.2 ± 47.5	62.5 ± 18.6	34.0 ± 5.9
Open time (%)	1.84 ± 0.37	3.55 ± 1.23	5.24 ± 0.71
Mean burst duration (msec)	3.90	10.75	6.55
Mean number of openings per burst	3.6	4.9	3.1
Number of openings	2895	4923	7863
Number of patches	5	4	5
Total time analyzed (sec)	316.2	265.0	245.4

Shown is a summary of kinetic properties of single channel GABAR currents evoked by 1, 3, and 10 μM GABA. Major kinetic properties of single channel openings are represented as the means and SEM for the number of patches indicated. The burst properties were determined from the pooled data from all analyzed patches.

shown), but the proportions shifted from shorter to longer burst durations (64.5, 22.5, and 12.8% for shortest to longest durations for 1 μM GABA vs 31.0, 28.2, and 40.6% for 3 μM GABA). There was an increase in mean burst duration from 3.9 at 1 μM GABA to 10.8 msec at 3 μM GABA, with a concomitant increase in mean openings per burst from 3.6 to 4.9 (Table 1). At 10 μM GABA, however, mean burst duration and the number of openings per burst decreased to 6.6 and 3.1 msec, respectively, again probably because of entry into desensitized states from which recovery may be slow.

Pharmacology of GABAR currents

Individual NT2-N neurons were tested for their responsiveness to a variety of GABAR modulators. In each of the cells tested with all of the following drugs ($n = 3$), the positive allosteric modulators diazepam (300 nM), loreclezole (3 μM), and pentobarbital (100 μM) enhanced currents evoked by 10 μM GABA (Fig. 5*A*), whereas the negative allosteric modulators zinc (100 μM), bicuculline (100 μM), and picrotoxin (30 μM) inhibited currents evoked by 30 μM GABA (Fig. 5*B*). GABAR currents in NT2-N cells were further studied to characterize the pharmacology of NT2-N GABARs in greater detail with a variety of compounds that modulate GABAR function (Table 3).

Barbiturates

Both pentobarbital (Fig. 6*A*) and phenobarbital (Fig. 6*B*) enhanced whole-cell GABAR currents evoked by 10 μM GABA. Pentobarbital maximally enhanced GABA-evoked currents by 434 ± 60% at 200 μM ($n = 6$) with an apparent EC_{50} of 41.3 μM and Hill slope of 1.47 (Fig. 6*C*). Phenobarbital maximally enhanced GABAR current to 331 ± 37% of control at 3 mM but was ~10-fold less potent with an apparent EC_{50} of 412 μM and a Hill slope of 2.21 ($n = 5$) (Fig. 6*C*).

Benzodiazepines

Diazepam (300 nM) enhanced whole-cell GABAR currents evoked by 10 μM GABA (Fig. 7*A*). Diazepam maximally enhanced GABAR current to 340 ± 42% ($n = 5$) of control at 100 nM diazepam with an apparent EC_{50} of 74.2 nM and a Hill slope of 1.08 (Fig. 7*D*). Concentration–response curves were obtained in five cells by coapplication of diazepam with 10 μM GABA.

Zolpidem

The imidazopyridine zolpidem is another GABAR benzodiazepine site agonist sensitive to the α subunit subtype. Zolpidem (10 μM) enhanced GABAR currents evoked by 10 μM GABA in all but one of the NT2-N cells studied (eight of nine) (Fig. 7*B*). Zolpidem enhanced GABAR currents with moderate affinity when coapplied with 10 μM GABA (EC_{50}, 527 nM; Hill slope, 0.99) (Fig. 7*D*).

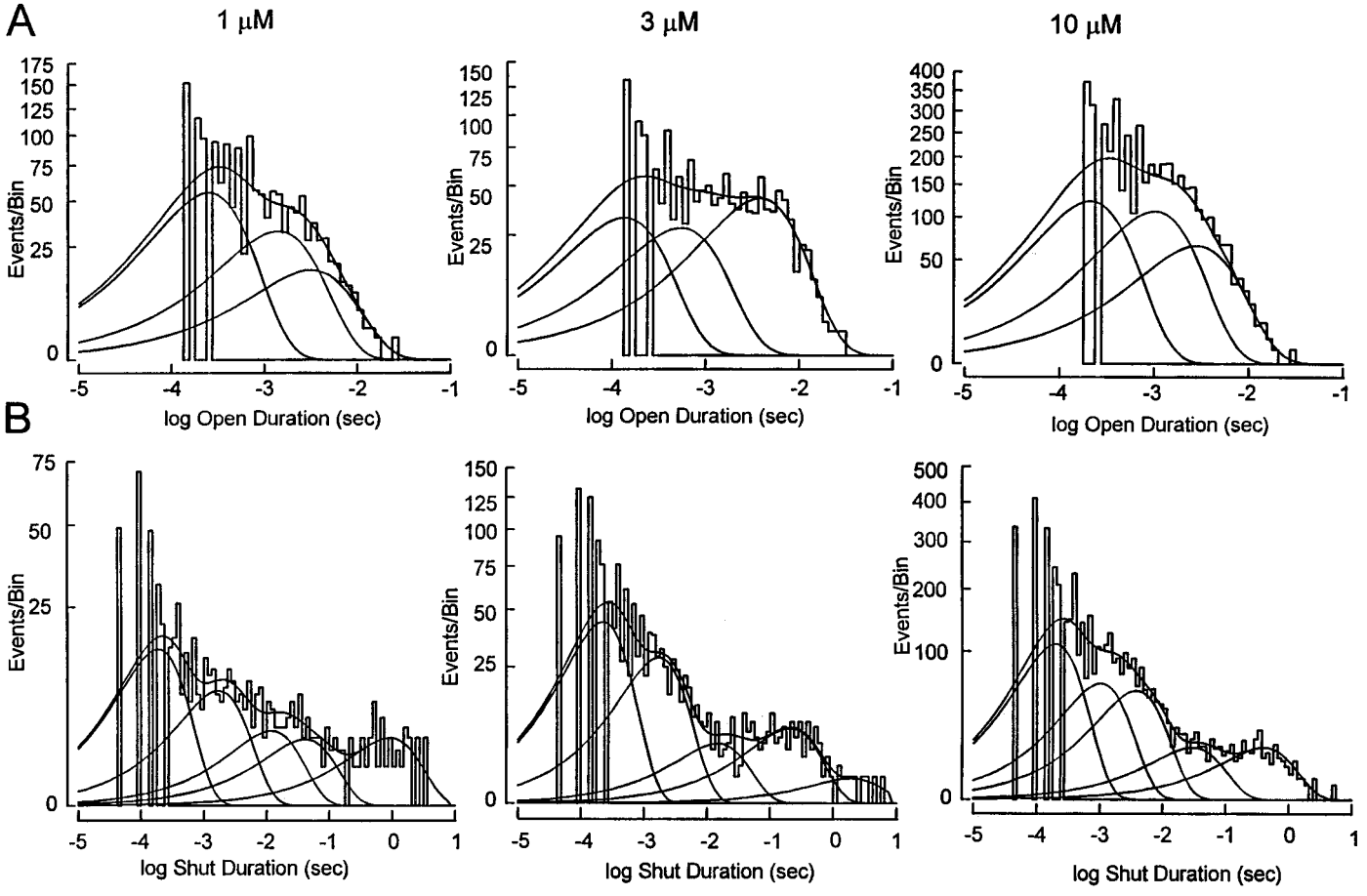

Figure 4. Open and closed histograms of single-channel currents evoked by 1, 3, and 10 μM GABA. *A*, Open-duration histograms for a single patch exposed to 1, 3, and 10 μM GABA. Open times were best fit by three exponential distributions with time constants and proportions as reported in Table 2. *B*, Closed-duration histograms for a single patch exposed to 1, 3, and 10 μM GABA. Closed times were best fit by five exponential distributions with time constants and proportions as reported in Table 2.

DMCM

DMCM is a β-carboline that acts as an inverse agonist at the benzodiazepine site. DMCM (3 μM) reduced whole-cell GABAR currents evoked by 30 μM GABA (Fig. 7*C*). DMCM produced a maximal reduction of 44.6 ± 5.2% of GABAR current (n = 9) with an IC_{50} of 44.8 nM and Hill slope of −1.12 (Fig. 7*D*). Eight of the nine cells tested showed inhibition of the current across the range of DMCM concentrations tested. However, in one cell GABAR currents were enhanced at concentrations up to 30 nM and inhibited at higher concentrations.

Table 2. Open and closed time constants and relative proportions

	GABA (1 μM)		GABA (3 μM)		GABA (10 μM)	
	Mean ± SEM	% events	Mean ± SEM	% events	Mean ± SEM	% events
Open τ (msec)						
τ1	0.28 ± 0.064	57 ± 2	0.21 ± 0.04	46 ± 8	0.25 ± 0.01	45 ± 4
τ2	1.54 ± 0.08	23 ± 5	1.08 ± 0.33	32 ± 4	2.09 ± 0.49	37 ± 7
τ3	4.49 ± 0.47	12 ± 3	4.92 ± 1.00	23 ± 9	4.18 ± 0.54	18 ± 3
Closed τ (μ sec)						
τ1	0.26 ± 0.08	50 ± 5	0.24 ± 0.01	50 ± 2	0.20 ± 0.02	44 ± 3
τ2	1.65 ± 0.60	23 ± 2	1.86 ± 0.11	30 ± 2	1.21 ± 0.14	31 ± 4
τ3	12.4 ± 3.5	10 ± 2	12.8 ± 2.6	9 ± 2	6.0 ± 0.96	16 ± 3
τ4	204 ± 95	11 ± 4	141 ± 54	8 ± 1	106 ± 53	5 ± 2
τ5	1617 ± 288	6 ± 2	1445 ± 386	4 ± 2	822 ± 200	4 ± 1

Open and closed time constants and proportions of openings for single channel GABAR currents evoked by 1, 3, and 10 μM GABA (derived from fits of GABAR main state open and closed duration histograms) are shown. Time constants (τ) for the open and closed time distributions (mean ± SEM) were derived from the averaged means of exponential fits of GABAR main state open- and closed-duration histograms created for each patch and GABA concentration. The proportion of openings fit by each exponential component represents the mean ± SEM for each component of similar τ at each GABA concentration.

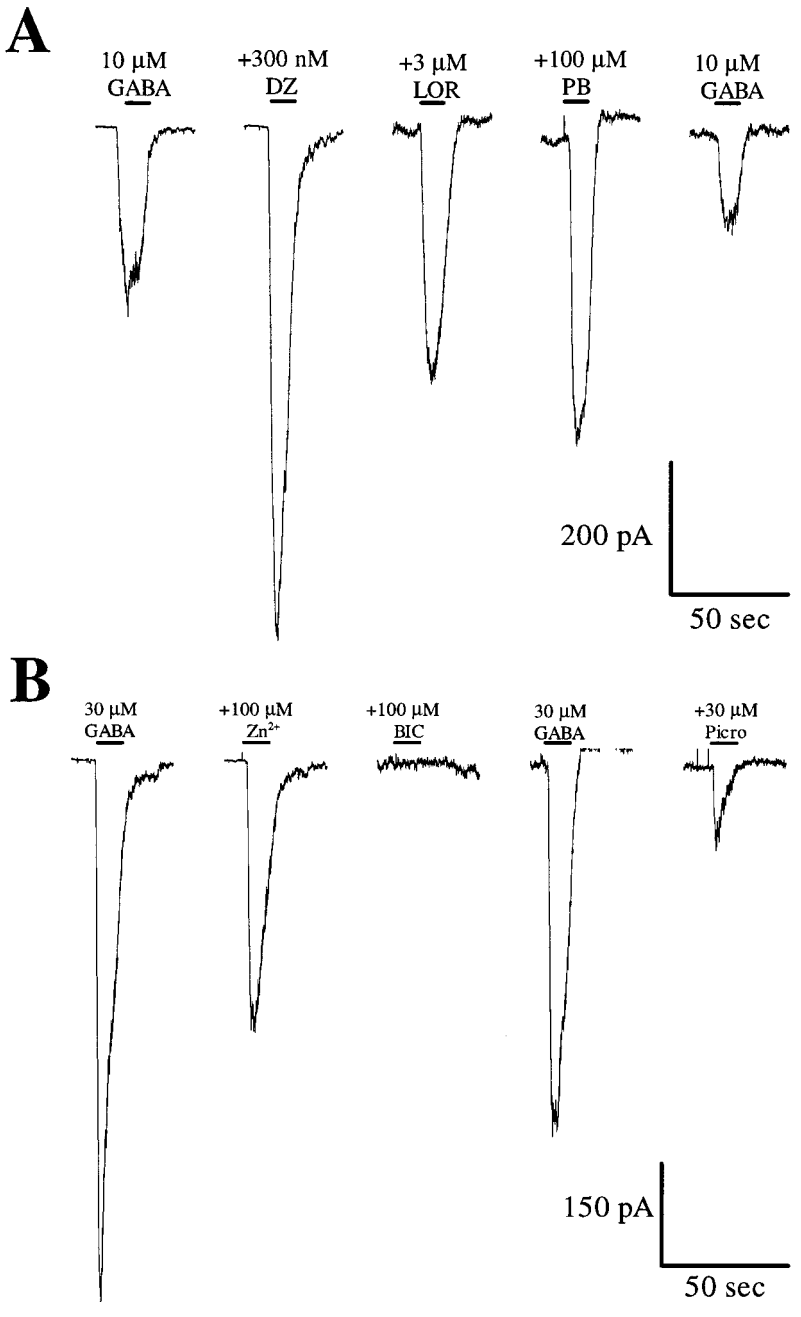

Figure 5. Pharmacological responses of an individual neuron to a variety of allosteric modulators that act at distinct GABAR sites. *A*, Coapplication of GABA plus positive allosteric modulators. Membrane currents were recorded in response to 10 μM GABA, followed by 10 μM GABA plus 300 nM diazepam (*DZ*), 3 μM loreclezole (*LOR*), and 100 μM pentobarbital (*PB*), and then 10 μM GABA alone. *B*, Coapplication of GABA with negative allosteric modulators recorded in the same neuron as shown in *A*. Current traces were recorded in response to 30 μM GABA, followed by GABA plus 100 μM zinc (Zn^{2+}), GABA plus 100 μM bicuculline (*BIC*), GABA alone, and finally 30 μM GABA plus 30 μM picrotoxin (*Picro*). *Horizontal bars*, Drug applications made at 2 min intervals.

Loreclezole

The novel anticonvulsant drug loreclezole interacts with a site on the β2 and β3 subtypes to enhance GABAR currents (Wafford et al., 1994). Loreclezole enhanced GABAR currents evoked by 10 μM GABA in every cell tested ($n = 5$) (Fig. 8*A*). Peak enhancement occurred at 10 μM loreclezole (240 ± 46%), but the degree of enhancement decreased at 30 μM loreclezole (148 ± 23%) for all five cells tested (Fig. 8), as previously reported for recombinant $\alpha5\beta3\gamma2$ GABARs (Donnelly and Macdonald, 1996). To determine the EC_{50} for loreclezole, only the responses between 100 nM and 10 μM were used to generate the concentration–response relationship. Under these conditions, the loreclezole EC_{50} was 1.22 μM with a Hill slope of 3.26 ($n = 5$) (Fig. 8*B*).

Neurosteroids

Neurosteroids have been shown to differentially modulate GABAR currents. Alphaxalone (5α-pregnan-3α-ol-11,20-dione) and pregnenolone sulfate (5-pregnan-3β-ol-20-one sulfate sodium salt) are neurosteroids that enhance and inhibit GABAR currents, respectively. Alphaxalone (10 μM) enhanced currents elicited by GABA (10 μM) by 431 ± 31% ($n = 4$). Increasing concentrations of alphaxalone (30 nM to 30 μM) resulted in greater enhancement of the peak current (Fig. 9*A*). A concentration–response curve of the enhancement of peak GABAR current relative to control was fit with a four-parameter logistic equation yielding an apparent EC_{50} of 414 nM and a Hill slope of 0.94 (Fig. 9*B*). Pregnenolone sulfate (10 pM to 10 μM) decreased GABAR currents (Fig. 9*C*) in a

Table 3. Summary of NT2-N cell GABAR pharmacology

	n	EC_{50}/IC_{50}	Hill slope	Maximal effect (% control)	Significance
Pentobarbital	6	41.3 μM	1.47	434.3 ± 60.0	***
Phenobarbital	5	411.5 μM	2.21	331.5 ± 37.1	**
Diazepam	5	74.2 nM	1.08	340.0 ± 41.9	*
Zolpidem	9	527 nM	0.99	233.9 ± 15.9	*
DMCM	9	44.8 nM	−1.12	55.4 ± 5.2	***
Loreclezole	5	1.2 μM	3.26	240.0 ± 45.5	*
Alphaxalone	4	414.2 nM	0.94	430.9 ± 30.6	***
Pregnenolone	4	4.9 mM	−0.50	32.5 ± 1.9	**
Picrotoxin	8	NA	NA	28.5 ± 3.4	***
Bicuculline	5	1.1 μM	−0.72	11.7 ± 4.0	*
Furosemide	5	1.4 mM	−1.3	21.8 ± 1.2	*
Zinc	5	14.7 μM	−0.43	5.2 ± 1.7	**
Lanthanum	1	NA	NA	77.5 ± 4.8	**

Compounds are grouped based on their site of action and are placed in the order in which they are discussed in the Results section. All half-maximal concentrations were calculated with the logistic equation provided in the Materials and Methods section. Significance was determined by comparing control currents (either 10 or 30 μM GABA) to the peak enhancement or inhibition produced by each compound using a two-tailed paired *t* test.

*$p < 0.05$; **$p < 0.01$; ***$p < 0.001$.

NA, not applicable.

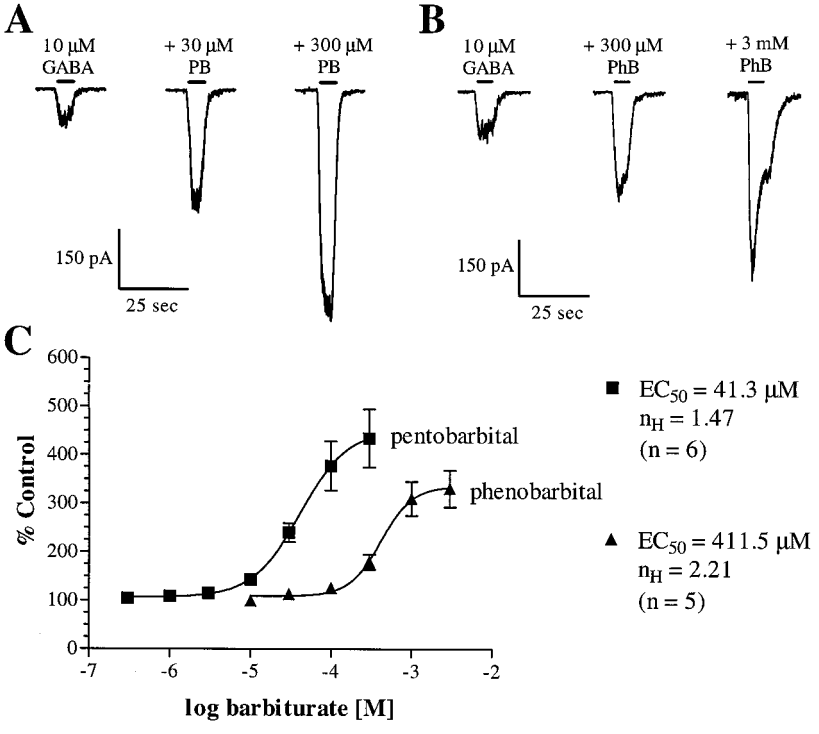

Figure 6. Enhancement of GABA-evoked currents by barbiturates with different affinities in NT2-N cells. *A*, Representative current traces showing current evoked by 10 μM GABA and enhancement by 30 and 300 μM pentobarbital (*PB*) (showing maximal enhancement). *B*, Representative current traces showing current evoked by 10 μM GABA and enhancement by 300 μM and 3 mM phenobarbital (*PhB*). *Horizontal bars*, Drug applications made at 2 min intervals. *C*, Concentration–response curves for enhancement of 10 μM GABAR peak currents by PB ($n = 6$) and PhB ($n = 5$). *Ordinate*, Percent of peak response to 10 μM GABA is displayed. Data are mean ± SEM.

concentration-dependent manner starting at 1 nM with a maximal inhibition of 67.5 ± 1.9% at 10 μM (Fig. 9*D*). An accurate IC_{50} for pregnenolone sulfate could not be calculated, because 10 μM was near the limit of solubility. However, fitting the data with a logistic equation where I_{max} was set at 0% yielded an equation with an apparent IC_{50} of 4.9 μM and a Hill slope of −0.50.

Bicuculline

Bicuculline is a competitive GABAR antagonist and has no effect on $GABA_B$ receptors, $GABA_C$ receptors, or the phylogenetically and structurally similar glycine receptor (Macdonald and Olsen, 1994). Bicuculline inhibits current at any functional GABAR isoform, irrespective of subunit composition. Currents evoked by

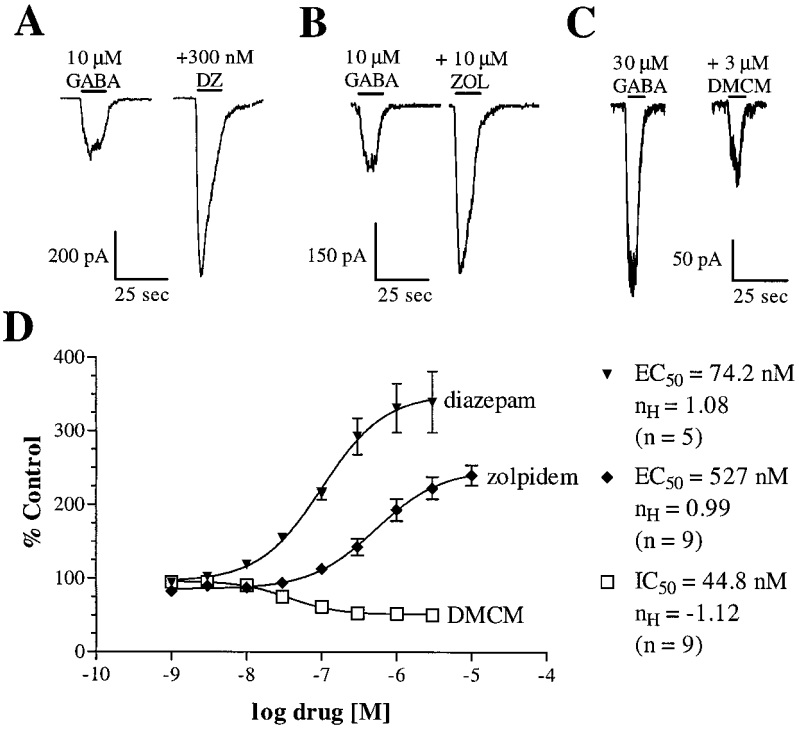

Figure 7. Benzodiazepine, imidazopyridine, and β-carboline modulation of NT2-N cell GABAR currents. *A–C*, Representative current traces from three different NT2-N cells showing maximal effect of three different modulators at the benzodiazepine site. The first pair of traces (*A*) shows control (10 μM *GABA*) and maximal enhancement by diazepam (*DZ*) (3 μM); the second pair (*B*) demonstrates 10 μM GABA control current and maximal enhancement by zolpidem (*ZOL*) (10 μM); and the third pair (*C*) shows the control response to 30 μM GABA followed by maximal inhibition by DMCM (3 μM). *Horizontal bars*, Drug applications made at 2 min intervals. *D*, Concentration–response relationships for enhancement of peak 10 μM GABAR currents by diazepam ($n = 5$) and zolpidem ($n = 9$) and inhibition of 30 μM GABAR currents by DMCM ($n = 9$). *Ordinate*, Percent of peak response to 10 μM GABA (diazepam or zolpidem) or 30 μM (*DMCM*). Data are mean ± SEM.

30 μM GABA in NT2-N cells were inhibited by bicuculline (10 nM to 30 μM) (EC_{50}, 1.1 μM; Hill slope, −0.72) (Fig. 10*A,C*). Currents elicited by 30 μM GABA were completely blocked by coapplication of 100 μM bicuculline.

Furosemide

Furosemide, an anthranilic acid derivative, inhibits recombinant GABAR currents with IC_{50}s in the micromolar range, but only when either an α4 or α6 subunit is present (Wafford et al., 1996). Furosemide (10 μM to 3 mM) inhibited NT2-N GABAR currents evoked by 30 μM GABA only at concentrations >100 μM (Fig. 10*B*). The greatest inhibition observed was 78.2 ± 1.2% at 3 mM furosemide; concentrations >3 mM could not be achieved because of limits of solubility; hence, true maximal inhibition could not be assessed. However, fitting the data with a logistic equation where I_{max} was set at 0% produced an apparent IC_{50} of 1.4 mM and a Hill slope of −1.3 (Fig. 10*C*).

Picrotoxin

Picrotoxin, a noncompetitive GABAR antagonist, also inhibited NT2-N GABAR currents. Picrotoxin (30 μM) blocked 71.5% of the peak current evoked by 30 μM GABA ($n = 8$) (data not shown). A complete concentration–response curve was not generated because of the long-lasting effects of moderate concentrations of picrotoxin (Table 3).

Polyvalent cations

The divalent cation zinc (Zn^{2+}) is a noncompetitive antagonist of GABAR currents. Zn^{2+} (300 nM) reduced whole-cell GABAR currents evoked by 30 μM GABA (Fig. 11*A*). Inhibitory concentration–response curves were generated by increasing the concentration of Zn^{2+} (100 nM to 1 mM) coapplied with a concentration of GABA near the EC_{50} for NT2-N cells (30 μM) (Fig. 11*C*). The IC_{50} for Zn^{2+} was 14.7 μM with a Hill slope of −0.43 ($n = 5$). GABAR currents were almost completely blocked by 1 mM Zn^{2+} (94.8 ± 1.7%).

The trivalent cation lanthanum (La^{3+}), when coapplied with a GABA concentration near the EC_{50}, inhibits α6-containing GABARs and enhances α1-containing GABARs (Saxena et al., 1997). La^{3+} (100 nM to 1 mM) was coapplied with either 10 μM (data not shown) or 30 μM GABA to NT2-N cells (Fig. 11*B*). La^{3+} had little effect on peak GABAR currents elicited by either GABA concentration. There were no statistically significant changes at lower La^{3+} concentrations. A small (22.5 ± 4.8%) but significant inhibition of GABAR currents evoked by 30 μM GABA was seen at 1 mM La^{3+} ($n = 11$) (Fig. 11*C*).

Distribution of maximal effects on individual neurons

The pharmacological data for the allosteric modulators that were tested are summarized in Table 3. The maximal effect was statistically compared with control GABA currents for each cell using paired *t* tests. Statistical significance was reached for each compound ($^*p < 0.05$; $^{**}p < 0.01$; and $^{***}p < 0.001$). Normalized maximal effects of all compounds tested on individual cells were evenly distributed around the mean and not separated into distinct groups.

PCR analysis of GABAR subunit mRNAs

Total RNA was isolated from cultures of NT2-N cells at the same 5 week time point that electrophysiological studies were performed. Reverse transcription PCR (RT-PCR) was used to determine the presence or absence of GABAR subunits using primers specific for human α1–6, β1–3, γ1–3, π, and ε subunit subtypes (Table 4). In repeated experiments, major bands were found for α2, α3, α5, β3, γ3, and π subtypes (Fig. 12), whereas bands for α1, β2, γ1, and γ2 subtypes were not found. Faint bands for the remaining subtypes (α4, α6, and β1) were inconsistently found. Primers designed to amplify the ε subunit did not amplify products of the predicted molecular size. Multiple primers were designed for the γ3 subtype. The molecular masses of the PCR products were slightly larger than the cDNA-positive control when the primers amplified the entire N-terminal domain to the

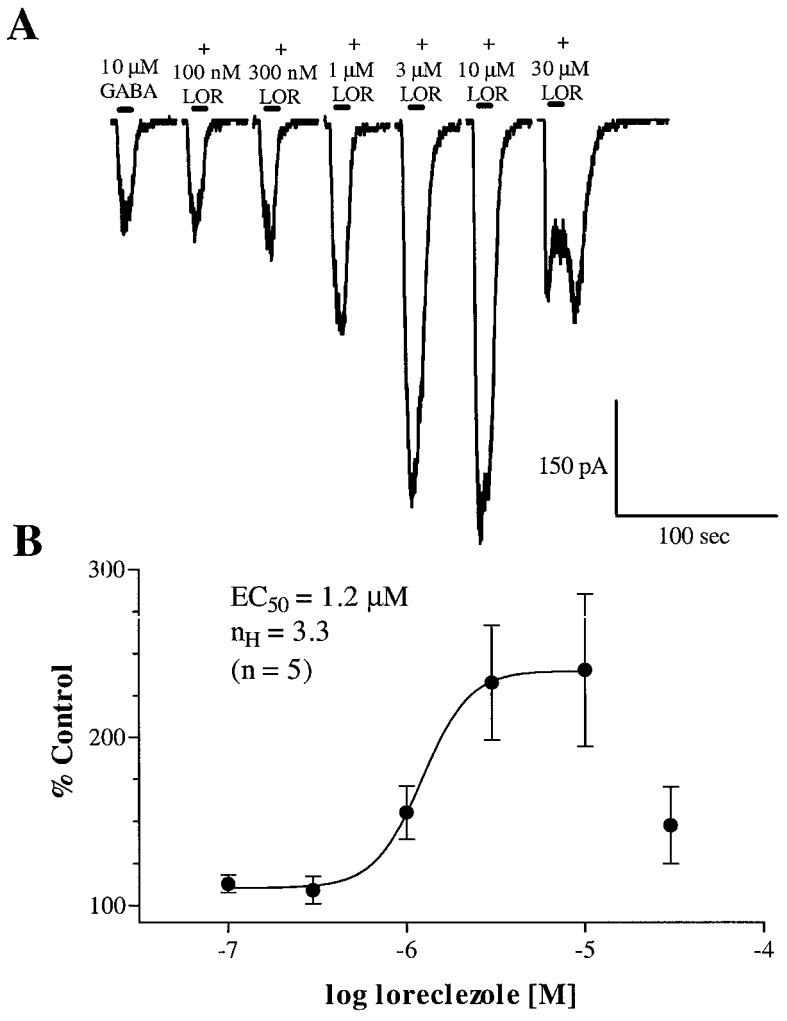

Figure 8. NT2-N cell GABAR current enhancement by loreclezole. *A*, Current traces from a single cell showing concentration-dependent enhancement of 10 μM GABAR currents by loreclezole (100 nM to 30 μM). Concentrations of loreclezole applied with 10 μM GABA are shown above the traces. *Horizontal bars*, Drug applications made at 2 min intervals. *B*, Loreclezole concentration–response relationship for GABAR current enhancement ($n = 5$). Data are mean ± SEM. The EC_{50} was derived from a four-parameter logistic equation fit to points up to 10 μM loreclezole. Inhibitory effects of higher concentrations of loreclezole were not investigated but may have reduced the maximal enhancement seen at 10 μM loreclezole and thus affected the calculated EC_{50}.

first intracellular loop [amino acids (aa) 18–267]. However, when the primers were designed to amplify only part of the N-terminal domain (aa 110) to midway through the large intracellular loop between M3 and M4 (aa 413), the PCR products were the same molecular mass as the cDNA control (data not shown). These same primers were unable to amplify either the γ1 or γ2 subtype, suggesting that the γ3 subtype expressed in NT2-N cells may represent a longer splice variant than previously described.

DISCUSSION

NT2-N cells express primarily α2, α3, α5, β3, γ3, and π GABARs subtype mRNAs

High mRNA levels for the α2, α3, α5, β3, γ3, and π subtypes were found using RT-PCR performed on total RNA isolated from NT2-N cells. Minimal mRNA levels for α4, β1, and γ1 subtypes were found in some, but not all, of the experiments, and no transcripts encoding human α1, α6, β2, or γ2 subtypes were detected. The pharmacological data suggested that a limited number of subunit subtypes were endogenously expressed in functional GABARs in NT2-N cells, which was confirmed by the use of RT-PCR. These subtype mRNAs were consistent with most of the pharmacological properties of GABAR currents recorded from NT2-N cells. Because RNA was isolated from an entire 10 cm dish of cells with no preference for cell type, we cannot rule out the possibility that there were subpopulations of NT2-N cells that expressed different isoforms based on either the stage of differentiation or differences in cell fate. It is unlikely that retinoic acid treatment alone would cause multiple fates of clonal NT2 stem cells. However, it is possible that multiple cell fates could occur during the differentiation process caused by secondary factors such as cell–cell or cell–substrate interactions that may alter the major GABAR isoforms being expressed. The possible existence of subpopulations of cells may also explain the low levels of α4, α6, and β1 mRNA and the inconsistency of their presence across RNA preparations. Although it is unlikely that NT2-N cells differentiate into a specific neuronal population found in the developing vertebrate brain, it is interesting to note that the subunits found expressed at high levels in NT2-N cells at this time point are located on chromosomes 15 (α5, β3, and γ3) and X (α3). With the exception of the α2 subtype mRNA, those barely detected were located on chromosome 4 (α2, α4, β1, and γ1), and those not expressed at all were located on chromosome 5 (α1, α6, β2, and γ2) (Rabow et al., 1995). The subunits expressed in NT2-N cells have been shown to be primarily expressed early in the development of the rat brain (Laurie et al., 1992), whereas those located on chromosome 5 are the predominate subunits found in adult rat brains (Wisden et al., 1992). NT2-N cells resemble immature CNS neurons, as determined by markers such as fetal τ, the incomplete phosphorylation state of high molecular weight neurofilament protein, and no MAP2b

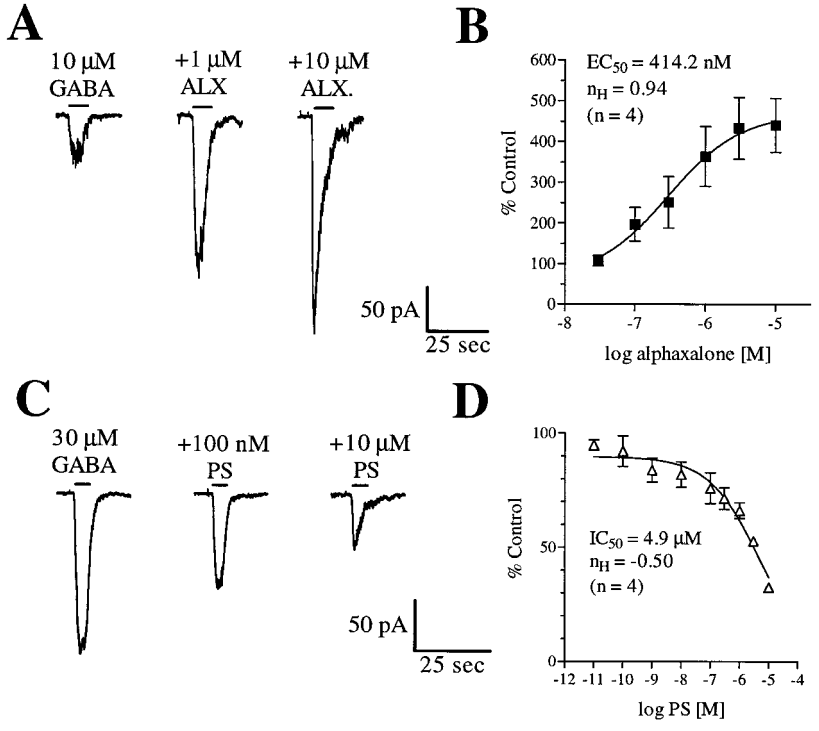

Figure 9. Modulation of NT2-N cell GABAR currents by neurosteroids. *A*, Representative current traces demonstrating enhancement of 10 μM GABAR currents by alphaxalone (*ALX*, 1 and 10 μM). *B*, ALX concentration–response relationship for GABAR current enhancement ($n = 4$). Data are mean ± SEM. *C*, Representative current traces of pregnenolone sulfate (*PS*) inhibition of 30 μM GABA-evoked currents at control levels (GABA alone), moderate inhibitory concentration (+100 nM PS), and maximal concentration (+10 μM PS). *D*, Pregnenolone sulfate concentration–response relationship for GABAR current inhibition ($n = 4$). Data are mean ± SEM. An apparent IC_{50} was calculated by a logistic equation where I_{max} was set at 0%.

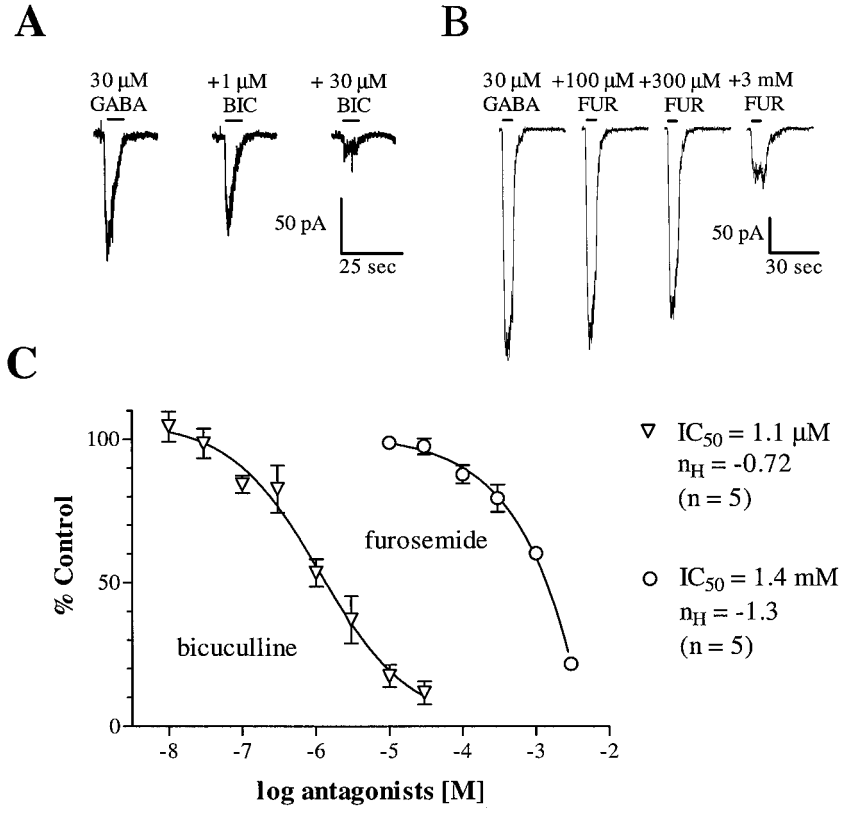

Figure 10. Inhibition of NT2-N cell GABAR currents by competitive (*BIC*) and noncompetitive (*FUR*) antagonists. *A*, Representative current traces of BIC inhibition of 30 μM GABA-evoked currents at control levels (GABA alone), IC_{50} concentration (+1 μM BIC), and a near maximal concentration (+30 μM BIC). *B*, Representative current traces of furosemide inhibition of 30 μM GABA-evoked currents at control levels (GABA alone), +100, 300 μM FUR and maximal concentration (+3 mM FUR). *C*, Concentration–response curves for inhibition of peak current amplitudes by BIC ($n = 5$) and FUR ($n = 5$). Either BIC or FUR was coapplied with 30 μM GABA. Data are mean ± SEM.

expression (Pleasure et al., 1992). Further studies are under way to determine whether all NT2-N cells contain all subtype mRNAs or whether there are multiple populations of cells with identifiable morphologies that contain different combinations of messages and whether the NT2 cell line undergoes a developmental switch in subunit expression similar to that found in rat brain.

NT2-N cells express GABARs likely composed primarily of α2, α3, α5, β3, and γ3 subtypes

Differentiated NT2-N neurons expressed GABARs with a distinct set of pharmacological and biophysical properties and expressed a limited number of GABAR subtype mRNAs. High

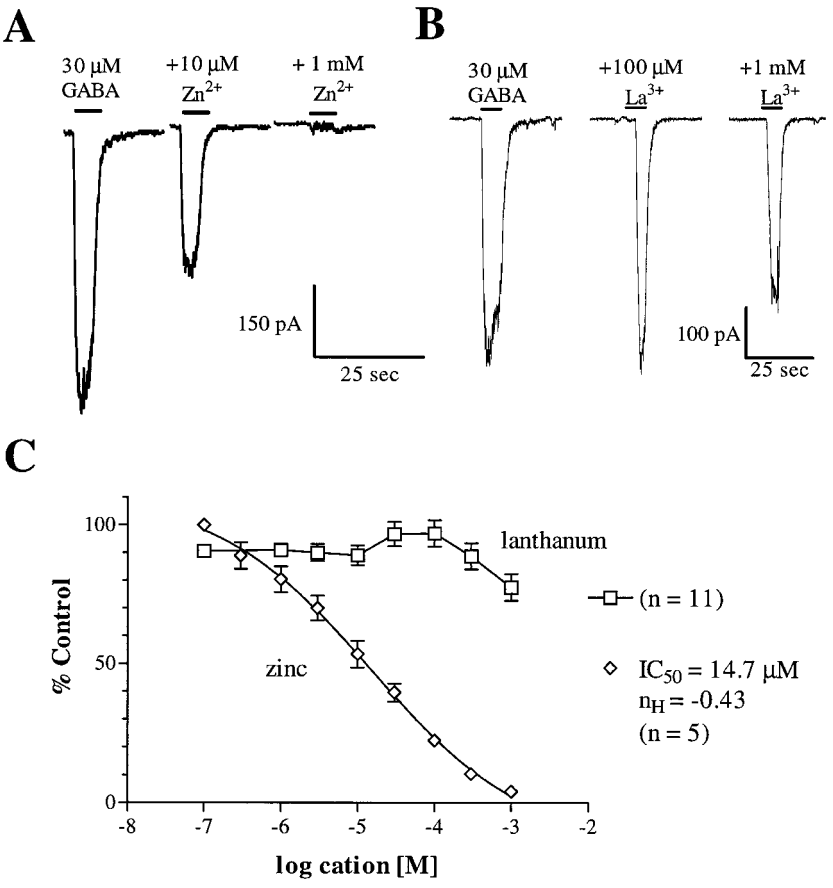

Figure 11. Effects of polyvalent cations on GABAR currents. *A*, Representative current traces of Zn^{2+} inhibition of 30 μM GABA-evoked currents at control levels (GABA alone), IC_{50} concentration (+10 μM Zn^{2+}), and maximal concentration (+1 μM Zn^{2+}). *B*, Representative current traces of La^{3+} inhibition of 30 μM GABA-evoked currents at control levels (GABA alone), +100 μM La^{3+} and maximal concentration (+1 mM La^{3+}). *Horizontal bars*, Drug applications made at 2 min intervals. *C*, Concentration–response curves for the effects of the polyvalent cations Zn^{2+} ($n = 5$) and La^{3+} ($n = 11$) on peak current amplitudes. Either Zn^{2+} or La^{3+} was coapplied with 30 μM GABA. Data are mean ± SEM.

levels of $\alpha 2$, $\alpha 3$, $\alpha 5$, $\beta 3$, $\gamma 3$, and π subunit subtype mRNAs were consistently amplified using RT-PCR performed on total RNA isolated from NT2-N cells. These data suggest that NT2-N cells express a limited number of GABAR isoforms with relatively uniform biophysical and pharmacological properties. NT2-N cells constitute the only known human-derived clonal cell line that express functional GABARs; therefore, they provide a unique preparation for investigation of human GABAR expression, assembly, structure, and regulation.

Studies using nonhuman recombinant GABAR subunits have shown that the affinity and efficacy for many GABAR modulators, as well as certain biophysical properties, depend on the expressed isoform. Although no definitive conclusions about the subunit subtype composition of GABARs can be made by determination of pharmacology and kinetic properties, several pharmacological and biophysical properties of NT2-N GABARs limit the possible expressed subtypes. Possible subtypes can be further limited by comparison of the pharmacological, biophysical, and RT-PCR data.

All NT2-N cells responded to GABA with a mean GABA EC_{50} of 21.8 μM, and individual EC_{50} values and maximal peak amplitudes were evenly distributed around the mean. Recombinant GABARs expressing rat or bovine α, β, and γ subunits had EC_{50} values ranging from 1–50 μM, whereas GABARs expressing $\alpha\beta\epsilon$, $\alpha\beta\delta$, or $\alpha\beta$ subunits alone had lower GABA EC_{50} values, ranging from 0.5 to 5 μM (Angelotti et al., 1993; Saxena and Macdonald, 1994) (T. R. Neelands and R. L. Macdonald, unpublished results). Thus, NT2-N cell GABARs had a GABA EC_{50} that was consistent with an isoform containing α, β, and γ subunits.

NT2-N GABARs likely contain a $\gamma 3$ subtype

Enhancement of GABAR currents by benzodiazepine site ligands requires the presence of a γ subunit in the receptor (Knoflach et al., 1991; Luddens et al., 1994; Hadingham et al., 1995; Benke et al., 1996). Because NT2-N cells expressed high levels of mRNA for $\gamma 3$, but not $\gamma 1$ or $\gamma 2$ subtypes, and GABAR currents were enhanced by diazepam, zolpidem, and reduced by DMCM, it is likely that NT2-N GABARs contain a $\gamma 3$ subtype.

NT2-N GABARs likely contain $\alpha 2$ and/or $\alpha 3$ subtypes

Recombinant GABARs with high affinity for benzodiazepines contain the $\alpha 1$ subtype, and low-affinity receptors contain either $\alpha 4$ or $\alpha 6$ subtypes when coexpressed with β and γ subtypes. Receptors with moderate affinity for diazepam can be further divided based on moderate affinity ($\alpha 2$- or $\alpha 3$-containing receptors) or insensitivity ($\alpha 5$-containing receptors) to zolpidem. In addition, DMCM, an inverse agonist at the benzodiazepine site, inhibited GABARs containing $\alpha 1$, $\alpha 2$, $\alpha 3$, and $\alpha 5$ subtypes but enhanced GABARs containing $\alpha 4$ and $\alpha 6$ subtypes. Furosemide is a high-affinity antagonist of recombinant rat GABARs that contain either $\alpha 4$ or 6 subtypes (Wafford et al., 1996) when coexpressed with γ and $\beta 2$ or $\beta 3$, but not $\beta 1$, subtypes (Korpi et al., 1995). The cation lanthanum enhances $\alpha 1$-containing receptors but inhibits $\alpha 6$-containing GABARs (Saxena et al., 1997) when coexpressed with a β and γ or δ subunit. The α subtype alters the magnitude and affinity of zinc block. GABARs containing $\alpha 2$ and $\alpha 3$ subtypes were blocked by zinc to a greater extent but with lower affinity than GABARs containing the $\alpha 1$ subtype (White and Gurley, 1995).

GABAR currents evoked from NT2-N cells were potenti-

Table 4. RT-PCR primers

Subunit	Fragment size (bp)		Start	5′ Sequence 3′	End
hGABAR α-1	470	Upper	664	GGA CAA ACA GTA GAC TCT GG	684
		Lower	1111	ATT AGG GGT GTA GCT GGT TGC TGT	1134
hGABAR α-2	471	Upper	661	CTG GGC CAA TCA ATC GGA AAG GAG A	585
		Lower	1108	GAT TCG GGG CAT AAT TGG CAA CAG C	
hGABAR α-3	470	Upper	734	TTT TGG GCC ATG TTG TTG GGA CAG AGA T	761
		Lower	1177	TGG TCC CCA CGA TGT TGA AGG TAG TGC T	1204
hGABAR α-4	554	Upper	928	TTG CCC AAA GTG TCC TAT GC	947
		Lower	1459	AGC CCC TAT GGT ATT AAC TGT GGT	1482
hGABAR α-5	570	Upper	86	GCT TTT CAC AGA TGC CAA CCA GTT CAG	112
		Lower	630	CCA TCT TCC GCC ACC ACC ACC GAC TTG	656
hGABAR α-6	471	Upper	634	GGA CAA ACA GTA TCT AGT GAG AC	656
		Lower	1086	GAT ATT TGG AGT CAG GAT GC	1105
hGABAR β-1	542	Upper	651	GAT GGT GTC TAA GAA GGT GGA G	672
		Lower	1170	TCA TAG GAG TAC ATG GTG GCC TTG	1193
hGABAR β-2	433	Upper	571	TAC TGG CGT GGC GAT GAT AAT G	592
		Lower	1004	GGC CCC CTC CCA AAG AAG A	986
hGABAR β-3	794	Upper	279	AGA TAA AAG GCT CGC CTA TTC TGG	302
		Lower	1050	CTT TCG CTC TTT GAA CGG TCA TTC	1073
hGABAR γ-1	465	Upper	735	CTC AAC TGA AAT CAT TCA CAC G	756
		Lower	1180	ATC TTC TTG CGG CAC AGA AAT	1200
hGABAR γ-2	558	Upper	754	GTG AAG ACA ACT TCC GG	770
		Lower	1288	CCA AGC TCC TGT TCG ACA ATC TTC	1311
hGABAR γ-3	769	Upper	56	CAG AAA GGT GGA AGA GGA TGA A	78
		Lower	802	AAA TGA CAC CCA GGA TAA AAC CAC	825
hGABA ϵ	314	Upper	34	CGC GGA AAT GTT GTC CAA AGT TCT	57
		Lower	328	CGG CGA TCT CAA CAG TGA CC	347
hGABAR π	591	Upper	84	CGA GGT CGG CAG AAG TGA CAA G	105
		Lower	652	TCC TGC TGC GAT CTG GTG ACT AA	674

Primers used to direct PCR amplification of human GABAR mRNAs expressed in NT2-N cells and the cDNA positive controls. The sequences of the primer pairs used to amplify each subunit, the fragment size (in base pairs), and the region amplified were included.

ated by both diazepam and zolpidem with only moderate affinity, suggesting the presence of an α2 and/or α3 subtype. DMCM inhibited GABAR currents with a moderate affinity; furosemide blocked GABAR current with low affinity; lanthanum had no significant effect on the currents; and zinc had an apparent affinity of 14.7 μM, almost completely blocking (95%) the current at 1 mM, suggesting that the major isoform expressed in NT2-N GABARs did not contain α1, α4, and α6 subtypes. The zinc affinity was similar to that reported for dentate granule cell GABARs (28 μM; Kapur and Macdonald, 1996) and for α5β3γ2L receptors (22 μM; Burgard et al., 1996) but was higher than described for αβ combinations (~560 nM) (Draguhn et al., 1990). A combination of the subunits identified by RT-PCR (α2, α3, and/or α5, β3, and γ3) would be consistent with the effect of zinc as well as the potentiation by diazepam.

These data suggest that NT2-N cells might express α2 and/or α3 subtypes and likely do not express α1, α4, or α6 subtypes. The RT-PCR study demonstrated the presence of α5 in addition to α2 and α3 subtype mRNAs. Although α5 is expressed, the enhancement of NT2-N currents by zolpidem argues against incorporation of α5 into the major isoform expressed by NT2-N cells. Taken together, these data are consistent with the presence of α2 and/or α3 subtypes coassembled with β and γ subtypes.

NT2-N GABARs likely contain the β3 subtype

Loreclezole enhancement of recombinant rat GABARs acts at a specific modulatory site on the β2 and β3, but not β1, subtypes (Wingrove et al., 1994). In addition, when β1 and β3 were coexpressed, loreclezole sensitivity was similar to that of the low-affinity β1-containing isoforms (Donnelly and Macdonald, 1996). High levels of message for β3 in NT2-N cells with little or no message for β1 or β2 would predict high-affinity enhancement of GABA-evoked currents by loreclezole. GABA-evoked currents in NT2-N cells were enhanced by loreclezole with a calculated

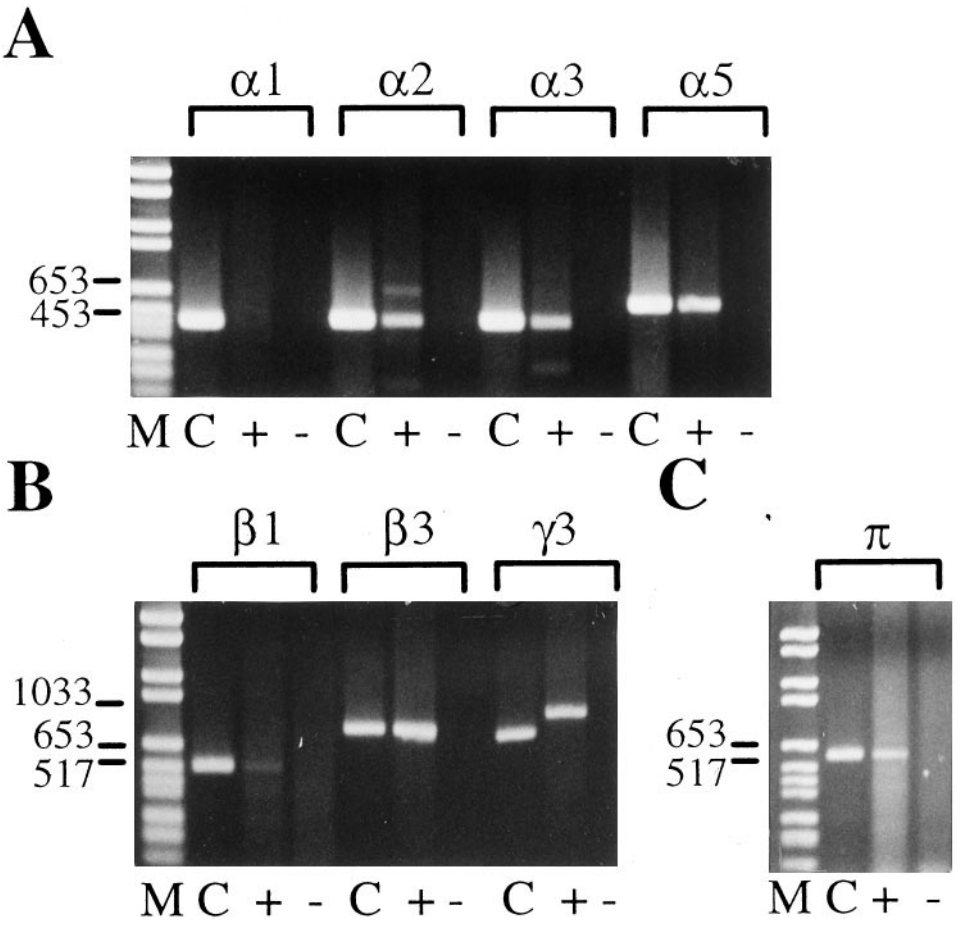

Figure 12. RT-PCR reaction amplification of GABAR subunits in NT2-N cells. *Lanes* are designated as follows: *M*, marker; *C*, human cDNA for each subunit subtype used as a positive control; +, NT2-N RNA with Superscript II; −, NT2-N RNA without Superscript II used as a negative control. *A*, Agarose gel of GABAR α subunits showing the presence of α2, 3, and 5 but not α1. (α*1*, *lanes 2–4*; α*2*, *lanes 5–7*; α*3*, *lanes 8–10*; α*5*, *lanes 11–13*; *lanes 1* and *14* are standards). *B*, Non-α subunits showing major bands for β3, γ3, and π but only a faint band for β1. (β*1*, *lanes 2–4*; β*3*, *lanes 5–7*; γ*3*, *lanes 8–10*; *lane 1* standard). *C*, Major band for the π subunit (π, *lanes 2–4*; *lane 1* standard). In some lanes, bands of lower molecular mass than that predicted for the product of interest, which are nonspecific PCR amplification products, were stained (Bloch, 1991).

affinity consistent with those previously reported for recombinant rat GABARs. These data, along with the RT-PCR findings, support the incorporation of only the β3 subtype into the major NT2-N GABAR isoform.

NT2-N GABAR biophysical properties were consistent with an α, β, and γ subunit subtype containing isoform

Single GABAR channels pulled from NT2-N cells opened in bursts to three different conductance levels: 19, 23, and 27 pS. These conductance levels were similar to those observed in native GABAR isolated in membrane patches from cultured mouse spinal neurons (Bormann et al., 1987) and cultured chick neuron patches (Weiss et al., 1988). Single-channel studies of recombinant rat GABARs have shown similar conductance levels of 29 and 21 pS for GABAR isoforms composed of α1, β1, and γ2S subunits but 15 and 10 pS for GABARs composed of α1 and β1 (Angelotti and Macdonald, 1993; Moss et al., 1990).

Kinetic analysis of the main conductance level openings suggested the presence of three open states and five closed states, similar to those determined in our laboratory for native GABAR channels in outside-out patches obtained from mouse spinal cord neurons in primary cell culture (Macdonald et al., 1989). A limited burst analysis showed concentration-dependent burst distributions similar to previously reported native and recombinant receptors. In most respects, however, the kinetic behavior of NT2-N single-channel GABAR openings was consistent with that reported in earlier studies.

Although studies of recombinant rat or bovine GABAR single-channel currents have not demonstrated a particular conductance level or kinetic "fingerprint" for specific isoforms, isoforms containing only an α and β subunit generally resulted in smaller single-channel conductance levels compared with γ-containing receptors and only two rather than three open states. To date no other detailed single-channel analysis has been done on human recombinant receptors or native isoforms from human tissue. Therefore, because this is the first single-channel description of human GABARs, only limited comparisons can be made between this study and previous work. However, the single-channel currents of NT2-N cells are remarkably similar in the pattern and level of their openings to other native GABA receptors and are consistent with the RT-PCR and pharmacological results, suggesting that the native NT2-N GABAR is composed of an α, β, and γ subunit.

REFERENCES

Abraham I, Sampson KE, Powers EA, Mayo JK, Ruff VA, Leach KL (1991) Increased PKA and PKC activities accompany neuronal differentiation of NT2/D1 cells. J Neurosci Res 28:29–39.

Andrews PW (1984) Retinoic acid induces neuronal differentiation of a cloned human embryonal carcinoma cell line *in vitro*. Dev Biol 103:285–293.

Angelotti TP, Macdonald RL (1993) Assembly of $GABA_A$ receptor subunits: α1 β1 and α1 β1 gamma2S subunits produce unique ion channels with dissimilar single-channel properties. J Neurosci 13:1429–1440.

Angelotti TP, Uhler MD, Macdonald RL (1993) Assembly of $GABA_A$ receptor subunits: analysis of transient single-cell expression utilizing a fluorescent substrate/marker gene technique. J Neurosci 13:1418–1428.

Beczkowska IW, Gracy KN, Pickel VM, Inturrisi CE (1997) Inducible expression of *N*-methyl-D-aspartate receptor, and delta and mu opioid

receptor messenger RNAs and protein in the NT2-N human cell line. Neuroscience 79:855–862.
Benke D, Honer M, Michel C, Mohler H (1996) $GABA_A$ receptor subtypes differentiated by their gamma-subunit variants: prevalence, pharmacology and subunit architecture. Neuropharmacology 35:1413–1423.
Bloch W (1991) A biochemical perspective of the polymerase chain reaction. Biochemistry 30:2735–2747.
Bormann J, Hamill OP, Sakmann B (1987) Mechanism of anion permeation through channels gated by glycine and gamma-aminobutyric acid in mouse cultured spinal neurones. J Physiol (Lond) 385:243–286.
Burgard EC, Tietz EI, Neelands TR, Macdonald RL (1996) Properties of recombinant gamma-aminobutyric acid A receptor isoforms containing the α 5 subunit subtype. Mol Pharmacol 50:119–127.
Colquhoun D, Sakmann B (1985) Fast events in single-channel currents activated by acetylcholine and its analogs at the frog muscle end-plate. J Physiol (Lond) 369:501–557.
Davies PA, Hanna MC, Hales TG, Kirkness EF (1997) Insensitivity to anesthetic agents conferred by a class of GABA(A) receptor subunit. Nature 385:820–823.
Donnelly JL, Macdonald RL (1996) Loreclezole enhances apparent desensitization of recombinant $GABA_A$ receptor currents. Neuropharmacology 35:1233–1241.
Draguhn A, Verdorn TA, Ewert M, Seeburg PH, Sakmann B (1990) Functional and molecular distinction between recombinant rat GABAA receptor subtypes by Zn^{2+}. Neuron 5:781–788.
Gibbs III JW, Zhang YF, Kao CQ, Holloway KL, Oh KS, Coulter DA (1996) Characterization of GABAA receptor function in human temporal cortical neurons. J Neurophysiol 75:1458–1471.
Greenfield LJJ, Macdonald RL (1996) Whole-cell and single-channel α1 β1 gamma2S $GABA_A$ receptor currents elicited by a "multipuffer" drug application device. Pflügers Arch 432:1080–1090.
Hadingham KL, Wafford KA, Thompson SA, Palmer KJ, Whiting PJ (1995) Expression and pharmacology of human $GABA_A$ receptors containing gamma 3 subunits. Eur J Pharmacol 291:301–309.
Hamill OP, Marty A, Neher E, Sakmann B, Sigworth FJ (1981) Improved patch-clamp techniques for high-resolution current recording from cells and cell-free membrane patches. Pflügers Arch 391:85–100.
Hartley RS, Lee VM (1997) Human N-Tera 2 neuronal (NT2N, hNT) cells are affected by astrocytes derived from different brain regions. Soc Neurosci Abstr 23:1420.
Hedblom E, Kirkness EF (1997) A novel class of GABAA receptor subunit in tissues of the reproductive system. J Biol Chem 272:15346–15350.
Horn R (1987) Statistical methods for model discrimination. Applications to gating kinetics and permeation of the acetylcholine receptor channel. Biophys J 51:255–263.
Kapur J, Macdonald RL (1996) Pharmacological properties of gamma-aminobutyric $acid_A$ receptors from acutely dissociated rat dentate granule cells. Mol Pharmacol 50:458–466.
Knoflach F, Rhyner T, Villa M, Kellenberger S, Drescher U, Malherbe P, Sigel E, Mohler H (1991) The gamma 3-subunit of the $GABA_A$-receptor confers sensitivity to benzodiazepine receptor ligands. FEBS Lett 293:191–194.
Korpi ER, Kuner T, Seeburg PH, Luddens H (1995) Selective antagonist for the cerebellar granule cell-specific gamma-aminobutyric acid type A receptors. Mol Pharmacol 47:283–289.
Kume A, Greenfield LJJ, Macdonald RL, Albin RL (1996) Felbamate inhibits [^{3}H]t-butylbicycloorthobenzoate (TBOB) binding and enhances Cl- current at the gamma-aminobutyric $Acid_A$ ($GABA_A$) receptor. J Pharmacol Exp Ther 277:1784–1792.
Laurie DJ, Wisden W, Seeburg PH (1992) The distribution of thirteen $GABA_A$ receptor subunit mRNAs in the rat brain. III. Embryonic and postnatal development. J Neurosci 12:4151–4172.
Luddens H, Seeburg PH, Korpi ER (1994) Impact of β and gamma variants on ligand-binding properties of gamma-aminobutyric acid type A receptors. Mol Pharmacol 45:810–814.
Macdonald RL, Olsen RW (1994) $GABA_A$ receptor channels. Annu Rev Neurosci 17:569–602.
Macdonald RL, Rogers CJ, Twyman RE (1989) Kinetic properties of the $GABA_A$ receptor main conductance state of mouse spinal cord neurones in culture. J Physiol (Lond) 410:479–499.
McManus OB, Magleby KL (1988) Kinetic states and modes of single large-conductance calcium- activated potassium channels in cultured rat skeletal muscle. J Physiol (Lond) 402:79–120.
Moss SJ, Smart TA, Porter NM, Nayeem N, Devine J, Stephenson FA, Macdonald RL, Barnard EA (1990) Cloned GABA receptors are maintained in a stable cell line: Allosteric and channel properties. Eur J Pharmacol 189:77–88.
Munir M, Lu L, Mcgonigle P (1995) Excitotoxic cell death and delayed rescue in human neurons derived from NT2 cells. J Neurosci 15:7847–7860.
Pleasure SJ, Page C, Lee VM (1992) Pure, postmitotic, polarized human neurons derived from NTera 2 cells provide a system for expressing exogenous proteins in terminally differentiated neurons. J Neurosci 12:1802–1815.
Pritchett DB, Sontheimer H, Shivers BD, Ymer S, Kettenmann H, Schofield PR, Seeburg PH (1989) Importance of a novel GABAA receptor for benzodiazepine pharmacology. Nature 338:582–585.
Rabow LE, Russek SJ, Farb DH (1995) From ion channels to genomic analysis: recent advances in GABAA receptor research. Synapse 21:189–274.
Saxena NC, Macdonald RL (1994) Assembly of $GABA_A$ receptor subunits: role of the δ subunit. J Neurosci 14:7077–7086.
Saxena NC, Neelands TR, Macdonald RL (1997) Contrasting actions of lanthanum on different recombinant gamma-aminobutyric acid receptor isoforms expressed in L929 fibroblasts. Mol Pharmacol 51:328–335.
Sigworth FJ, Sine SM (1987) Data transformations for improved display and fitting of single-channel dwell time histograms. Biophys J 52:1047–1054.
Twyman RE, Rogers CJ, Macdonald RL (1990) Intraburst kinetic properties of the $GABA_A$ receptor main conductance state of mouse spinal cord neurones in culture. J Physiol (Lond) 423:193–220.
Wafford KA, Bain CJ, Quirk K, McKernan RM, Wingrove PB, Whiting PJ, Kemp JA (1994) A novel allosteric modulatory site on the $GABA_A$ receptor β subunit. Neuron 12:775–782.
Wafford KA, Thompson SA, Thomas D, Sikela J, Wilcox AS, Whiting PJ (1996) Functional characterization of human gamma-aminobutyric acid A receptors containing the α 4 subunit. Mol Pharmacol 50:670–678.
Weiss DS, Barnes EMJ, Hablitz JJ (1988) Whole-cell and single-channel recordings of GABA-gated currents in cultured chick cerebral neurons. J Neurophysiol 59:495–513.
White G, Gurley DA (1995) α subunits influence Zn block of gamma 2 containing GABAA receptor currents. NeuroReport 6:461–464.
Wieland HA, Luddens H, Seeburg PH (1992) Molecular determinants in $GABA_A$/BZ receptor subtypes. Adv Biochem Psychopharmacol 47:29–40.
Wingrove PB, Wafford KA, Bain C, Whiting PJ (1994) The modulatory action of loreclezole at the gamma-aminobutyric acid type A receptor is determined by a single amino acid in the β2 and β3 subunit. Proc Natl Acad Sci USA 91:4569–4573.
Wisden W, Laurie DJ, Monyer H, Seeburg PH (1992) The distribution of 13 $GABA_A$ receptor subunit mRNAs in the rat brain. I. Telencephalon, diencephalon, mesencephalon. J Neurosci 12:1040–1062.
Younkin DP, Tang CM, Hardy M, Reddy UR, Shi QY, Pleasure SJ, Lee VM, Pleasure D (1993) Inducible expression of neuronal glutamate receptor channels in the NT2 human cell line. Proc Natl Acad Sci USA 90:2174–2178.